GEOLOGICA CARPATHICA, 47, 4, BRATISLAVA, AUGUST 1996
215–225

DISTRIBUTION OF Mn IN CARBONATES FROM THE UPPONY MTS., NE-HUNGARY

MÁRTA POLGÁRI and ISTVÁN FÓRIZS

Laboratory for Geochemical Research, Hungarian Academy of Sciences, Budaörsi út 45, H-1112 Budapest, Hungary

(Manuscript received June 14, 1995; accepted in revised form March 21, 1996)

Abstract: Microprobe analyses of metacherts from the Tapolcsány Metachert Member of the Tapolcsány Formation and of limestones from the Lázbérc Formation of the Uppony Mountains were completed to study Mn carbonate mineralization. The carbonate minerals in the metachert samples include calcite, siderite and ankerite, which contain variable but low amounts of Mn, with a mean Mn content of 0.83 weight percent. In one sample (No. 5), the Mn content is high, 8.15 weight percent, with the host mineral being Mn-rich ankerite. The limestone samples are composed of calcite and dolomite. Their iron and manganese contents are low, but somewhat higher in dolomite than in calcite. The environment of deposition of the Tapolcsány Metachert was euxine, with a high primary pyrite and organic matter content, which favoured a high dissolved manganese content. These conditions however, did not characterize the sedimentary environment of the Lázbérc Formation, which was more oxic.

In chronological order the original mineral composition underwent different changes: 1 — primary carbonate minerals included mostly small calcite (and rhodochrosite?) grains; 2 — regional-dynamothermal metamorphism probably changed the primary assemblage; 3 — Fe-Mg metasomatism caused changes due to its chemistry; small quantities of manganese were probably transported by the metasomatic fluids; 4 — surface weathering changed the original composition of the rocks; Fe and Mn was dissolved from the carbonates and Fe-Mn-oxide concentrations were formed in which the amount of Fe and Mn was much higher than in the pre-weathered rocks.

Key words: metasomatism, manganese, ankerite, siderite, calcite, dolomite, electron microprobe.

Introduction

Árkai (1983) outlined the broad geological framework of the area as follows: the thick Paleozoic-Mesozoic sequences of the NE Hungarian Bükk, Uppony, and Szendrő Mountains were deposited from Lower Devonian to the Jurassic, including several phases of the Hercynian cycle (Fig. 1). The sections occupy a characteristic megatectonic position: where they constitute the innermost zone of the Western Carpathians. These sections show stratigraphic, lithologic, and paleontological features similar to those of the Southern Alps and Internal Dinaride Mountains. During Alpine tectonism the formations were affected by folding, imbrication, and overthrusts.

Along the NE-SW trending Darnó megatectonic line, remarkable Fe-Mg metasomatism took place, the traces of which can be observed in the Aggtelek-Rudabánya Mountains (Koch et al. 1950; Pantó 1948, 1954, 1956); Uppony Mountains (Pantó 1954); Szendrő Mountains (Koch et al. 1950); and Darnó Hill (Kiss 1958), (Figs. 1 and 2a). As a result of the weathering of these deposits Fe-Mn oxide came to be concentrated on the surface.

Primary iron carbonate ores, always contain manganese that varies between 0.5–2.0 wt. %. Well-documented core samples are available from the Uppony Mountains, and consequently were investigated in detail.

The primary iron carbonate ore of the Uppony Mountains (metasomatized Guttenstein Dolomite) did not undergo metasomatism at its current tectonic position. The ore bodies are tectonic blocks moved from their original position by overthrust faulting (Árkai 1983). The sites of formation and tectonic blocks are unknown. The age of the manganese mineralization in the Paleozoic sections is not known.

The schematic geological map of the Uppony Mountains after Balogh (as presented in Árkai et al. 1981) is shown in Fig. 2a. Kovács (1984) divided the Uppony Mountains into

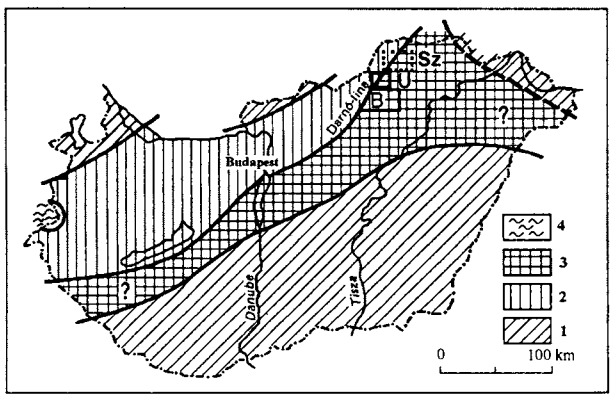

Fig. 1. Geological situation of the Uppony, Szendrő and Bükk Mountains. **1.** Medium- and low-grade polymetamorphic (Early Baikalian-Hercynian-Alpine) crystalline basement; **2.** very-low- and low-grade, generally Hercynian metamorphic Paleozoic basement with non-metamorphic Mesozoic; **3.** very-low- and low-grade metamorphic Paleozoic with very low-grade metamorphic Mesozoic (Alpine mobile belt); **4.** Penninicum of the Kőszeg Mountains; **SZ** = Szendrő Mountains; **U** = Uppony Mts.; **B** = Bükk Mts. (adopted from Árkai et al. 1981).

two large units. The first one consists mainly of clastic deposits situated in the southeastern part of the mountains (Tapolcsány Unit, including the Tapolcsány Metachert Member). The age of this member is debatable; Kozur & Mock (1973) assuming a continuous stratigraphic sequence suggested that it is Carboniferous, but on the basis of lithostratigraphic considerations, a Silurian age cannot be excluded (Kovács, Hungarian Geological Institute, oral communication, 1988).

The Tapolcsány Metachert Member consists of black metachert, manganiferous shale, and black radiolarite-bearing jasper, with metabasalt intercalations (Árkai 1978). The original sediment was a muddy-siliceous sequence of euxine facies with a high primary pyrite and organic matter content. In this geochemical environment, dissolved manganese content increased and precipitated when conditions became somewhat more oxidizing. Due to diagenesis and subsequent geological processes (regional dynamothermal metamorphism, metasomatism, weathering), manganese was partly mobilized and then the Mn-bearing minerals precipitated.

The second unit described by Kovács (1984) is the Uppony Unit (Lázbérc Formation) which constitutes the northwestern part of the mountains and consists for the most part of carbonate rocks intercalated by mudstone and sandstone layers. The limestone of the Lázbérc Formation is pale, banded or massive limestone of Middle Devonian age and of carbonate platform facies.

The Alpine regional tectonism that affected the Paleozoic rocks resulted in high-grade diagenesis and low-grade metamorphism (Árkai et al. 1981; Árkai 1983).

Materials and methods

Sample localities as well as mineralogical, petrological characteristics of samples are summarized in Tab. 1 and 2. Metachert samples were collected from drillcore Dt-8 (Fig. 2a), limestone samples from an outcrop (Fig. 2b).

Qualitative analyses were made by JEOL JXA-5 microprobe, quantitative measurements were carried out by JEOL Superprobe-733 microprobe equipped with EDAX. Polished sections of metachert and limestone were used in the analyses and quantitative analyses were made on different carbonate grains. Analytical conditions: accelerating voltage 20 kV; electron beam current 2.5 to 3.0 nA; 1–10 μm electron beam diameter; counting time 20 to 40 seconds. The standards used included MgO for Mg, calcite for Ca, hematite for Fe, and metallic manganese for Mn. The relative error of measurements was 5–8 percent. The peak overlapping of $Mn_{K\beta}$ and $Fe_{K\alpha}$ was corrected by the $Mn_{K\beta}/Mn_{K\alpha}$ ratio measured on the Mn-standard, where the $Mn_{K\beta}$ intensity was measured at the site of $Fe_{K\alpha}$.

Calcite decomposed not only under the focussed electron beam but also under the beam of 10 μm diameter. This indicates that the mineral was not compact and volatiles occur in micropores. The oxide sums for calcite analyses vary between 95 and 98 %. The missing 2–5 % is presumably bound water; this fact was taken into account in the interpretation.

Matrix correction was performed by the ZAF program (Nagy & Fórizs 1986) modified after Duncumb & Jones (1969).

Results

Tapolcsány Metachert Member

In all metachert samples several generations and types of carbonate minerals developed. Chemical compositions vary

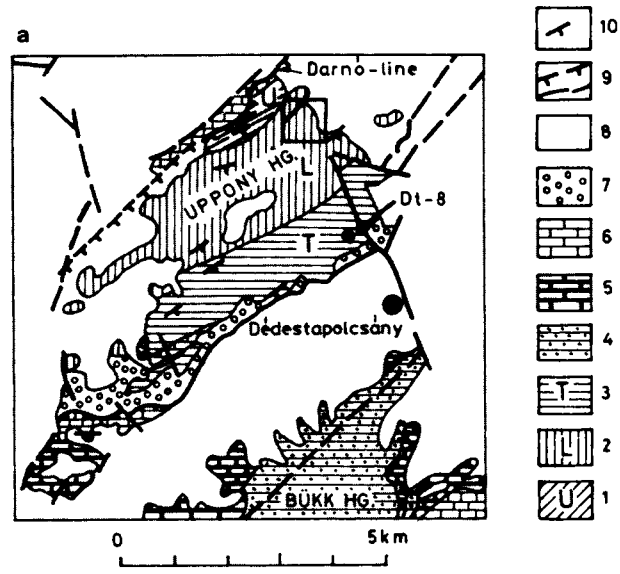

Fig. 2a. Geological sketch map of the Uppony Mountains (after Balogh, in: Árkai et al., 1981). **1** — Uppony Limestone; **2** — Lázbérc Formation; **3** — Tapolcsány Metachert; **4** — Middle-Upper Carboniferous (shale, sandstone, with limestone lenses); **5** — Permian (shale and sandstone, bituminous limestone); **6** — Triassic (dolomite, limestone, diabase-tuff); **7** — Cretaceous, Gosau conglomerate); **8** — Tertiary (sedimentary rocks); **9** — overthrust; **10** — fault.

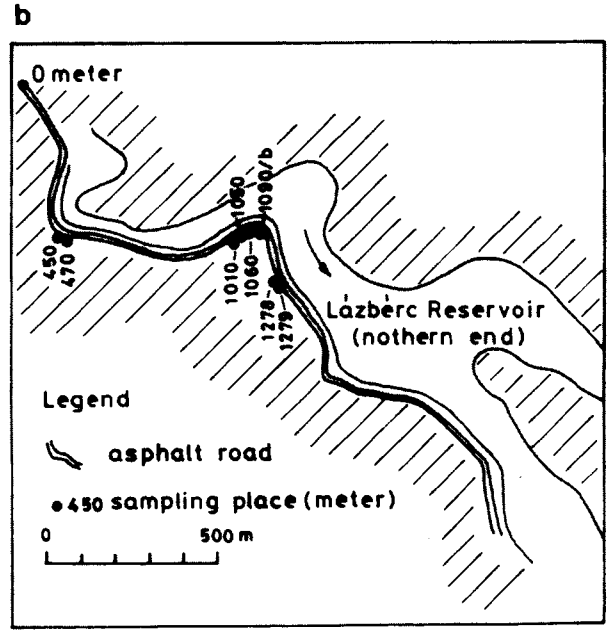

Fig. 2b. Location of sampling of Lázbérc Formation (Árkai 1978).

widely within the isomorphous series (calcite, ankerite, siderite; Fig. 3). In some samples the well-developed, more or less euhedral and in many places zoned carbonate minerals are frequent. In microprobe photos it is clear that in many places the carbonate grains fill micropores between quartz grains (Figs. 4a, b, c, d).

The carbonate grains are unoriented and dispersed, while the quartz grains are elongated and oriented as the result of

metamorphism. These petrographic relations indicate that the carbonate minerals formed subsequent to metamorphism.

The carbonate minerals were precipitated in micro-cracks and pores and display marked Fe-Mg zonation related to the temporal changes in composition of the mineralizing fluids. The core of the analyzed zoned carbonate minerals is of the same composition from grain to grain within the limits of error. The formation of zoned minerals reflect a non-equilibrium state. The occurrence and form (vein filling) of siderite also supports a ferrous metasomatic process; in an euxine environment siderite does not precipitate in the presence of sulphur but rather pyrite, with greater stability range forms in addition to rhodochrosite and manganiferous calcite (Hem 1972).

Disregarding one sample (No. 5) the Mn-content of carbonate minerals of the metachert member is low, and uniformly distributed. Representative microprobe analyses of chert samples containing manganiferous carbonate minerals as well as the mean manganese concentrations are summarized in Tab. 3.

The mean Mn content of ankerite and calcite of the metachert sample No. 1 is the same (0.85 wt. %), although the scatter of data is greater for ankerite. In calcite the manganese content exceeds that of both iron and magnesium. In some samples remarkable Mn concentrations were observed in ank-

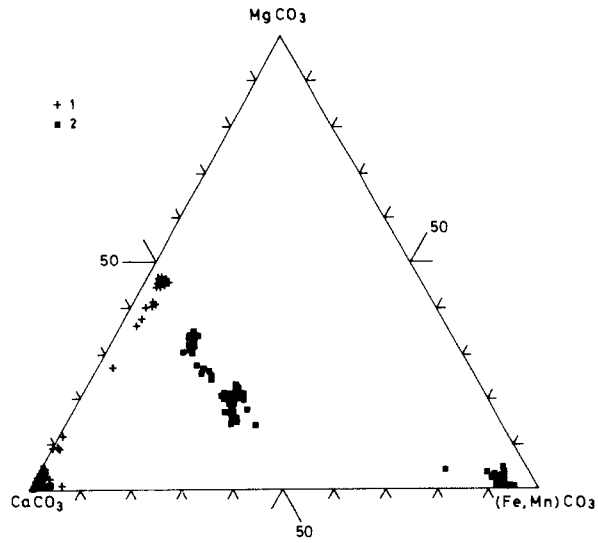

Fig. 3. $CaCO_3$-$MgCO_3$-$(Fe,Mn)CO_3$ ternary diagram of all carbonate analyses of samples of the Tapolcsány Metachert and Lázbérc Formation, in mole percent. **1** — Lázbérc Formation (Table 4); **2** — Tapolcsány Metachert (Table 3).

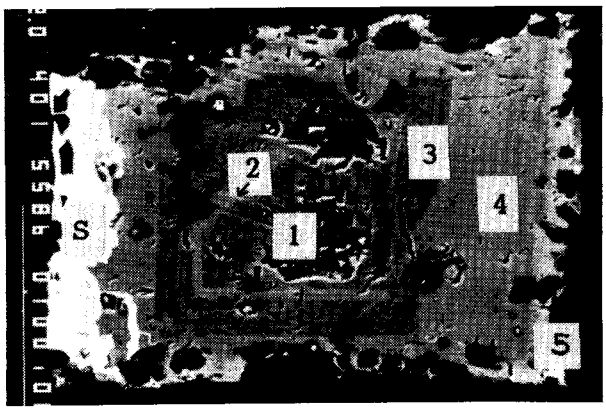

Fig. 4a. Backscattered electron image (Sample No. 2, corehole DT-8, 164.0 m). Siderite occurs at one margin of the zoned ankerite (white phase). For analyses of points see Table 3.

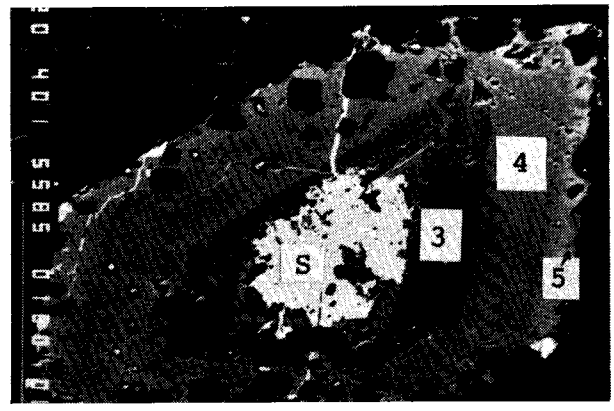

Fig. 4b. Backscattered electron image (Sample No. 2, corehole DT-8, 164.0 m). At the core of the zoned ankerite is siderite. For analyses of points see Table 3.

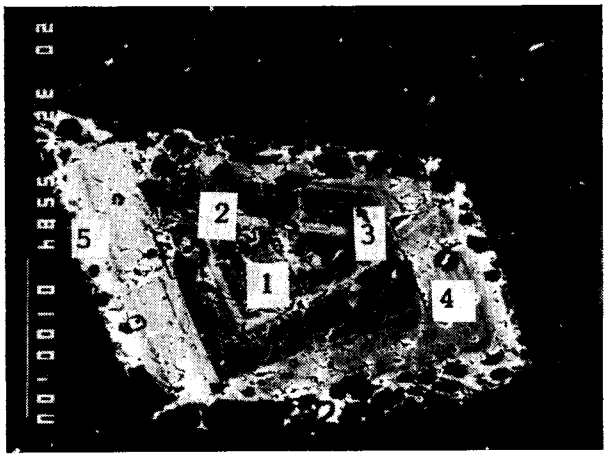

Fig. 4c. Backscattered electron image (Sample No. 2, corehole DT-8, 164.0 m). Zoned ankerite crystal in quartzite. The brighter parts of the grain are rich in Fe (type B). Analyses of points are in Table 3.

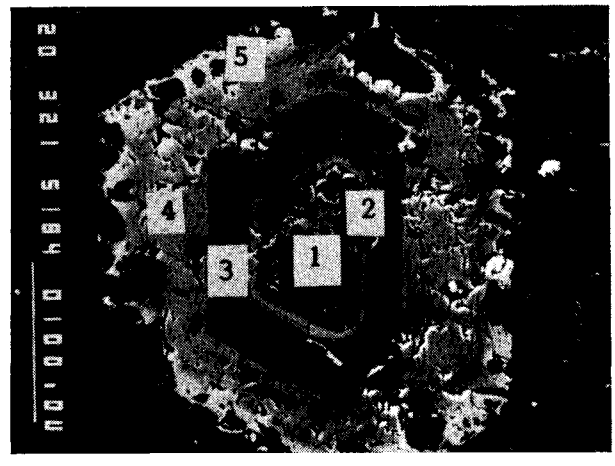

Fig. 4d. Backscattered electron image (Sample No. 2, corehole DT-8, 164.0 m). Zoned ankerite grain in quartzite. The brighter zones are rich in Fe (type B).

Table 1: Characteristics of metachert and limestone samples of the Uppony manganese deposits, Tapolcsány Formation, Tapolcsány Metachert Member (corehole DT-8).

No.	Corehole depth (Fig. 2a)	XRD mineralogy (Árkai 1978, and this study)	Mn phase	morphological features of carbonates	note
			--- based on microprobe investigations ---		
1.	DT-8 139.3 m	chlorite, quartz, K-feldspar, albite-oligoclase, sericite, ankerite-dolomite, calcite	calcite, ankerite	vein filling, disseminated	---
	DT-8 139.7 m	chlorite, quartz, K-feldspar, sericite, albite-oligoclase, pyrite ankerite-dolomite, siderite	calcite, ankerite	vein filling, disseminated	---
2.	DT-8 164.0 m	quartz, ankerite-dolomite, sericite, chlorite, siderite, pyrite, K-feldspar, albite-oligoclase	calcite, ankerite A, B,* siderite	zoned euhedral grains (ankerite, ankerite-siderite) vein filling (siderite), anhedral grains (siderite, calcite, ankerite A, B)	Zoned carbonates occur in a siliceous matrix, non-zoned grains occur with pyrite. Calcite and siderite occur in form of veins and as grains. Pyrite grains occur in the siderite-filled veins. In the ore, pyrrhotite and sphalerite can be distinguished.
3.	DT-8 165.3 m	quartz, ankerite-dolomite, sericite, chlorite, siderite, pyrite, K-feldspar, albite-oligoclase	ankerite, siderite	---	---
4.	DT-8 396.5 m	quartz, pyrite, albite-oligoclase, sericite, kaolinite, pyrite, ankerite-dolomite, siderite, chlorite, rutile	---	vein filling, anhedral	---
5.	DT-8 475.3 m	quartz, siderite, pyrite, sericite, ankerite-dolomite, chlorite, feldspar	Mn-rich, ankerite	euhedral grains, anhedral grains, disseminated	Euhedral minerals are found adjacent to the ore-bearing phases: pyrrhotite, sphalerite, pyrite.

*Ankerite A, B: explanation see in text.

Table 2: Characteristics of the metachert and limestone samples of the Uppony manganese deposit, Lázbérc Formation (outcrop samples).

No.	Sample* locality (Fig. 2b)	XRD mineralogy (Árkai 1978)	Mn phase	type of carbonates	morphological features of carbonates	note
			---------- based on microprobe investigations ----------			
1.	U 450 m	calcite, chlorite, sericite, quartz, hematite, K-feldspar	carbonate minerals	calcite	--	Vein network of hematite flakes and slightly oriented euhedral clay minerals in calcite.
2.	U 470 m	calcite, altered sericite	carbonate minerals	calcite	--	
3.	U 1010 m	ankerite-dolomite, calcite, sericite, quartz, hematite	carbonate minerals	ferrous dolomite, calcite	--	Calcite vein network.
4.	U 1050 m	calcite, ankerite-dolomite, sericite, feldspar, goethite, gypsum	carbonate minerals and Fe-Mn oxide phase	dolomite, calcite	--	Diagenesis, weathering, vein formation, Fe-Mn-oxides of heterogeneous composition, frequent thick veins with significant clay mineral and Fe contents.
5.	U 1060 m	ankerite-dolomite, calcite, sericite, quartz	carbonate minerals and Fe-Mn oxide phase	dolomite, calcite	--	Diagenesis, weathering, vein formation, Fe-Mn-oxides of heterogeneous composition, frequent thick veins with significant clay mineral and Fe contents.
6.	U 1090 m	ankerite-dolomite, calcite, sericite, quartz, chlorite feldspar, goethite	carbonate minerals and Fe-Mn oxide phase	calcite	--	Weathering, diagenesis.
7.	U 1278 m	ankerite-dolomite, calcite, quartz, sericite	carbonate minerals and Fe-Mn oxide phase	calcite, dolomite	Mn zoning is characteristic	Mn-zonation in calcite, Fe-Mn rhombohedral skeletons, traces of weathering, subsequent accumulations of Fe-Mn-oxides (hydroxides?).
8.	U 1279 m	ankerite-dolomite, calcite, quartz, sericite, kaolinite	carbonate minerals and Fe-Mn oxide phase	calcite, dolomite	Mn zoning, rarely calcite veins	Mn-zonation in calcite, Fe-Mn rhombohedral skeletons, traces of weathering, subsequent accumulations of Fe-Mn-oxides (hydroxides?).

*Being outcrop samples, the distances given in meters denote distance from a given point (0 meter).

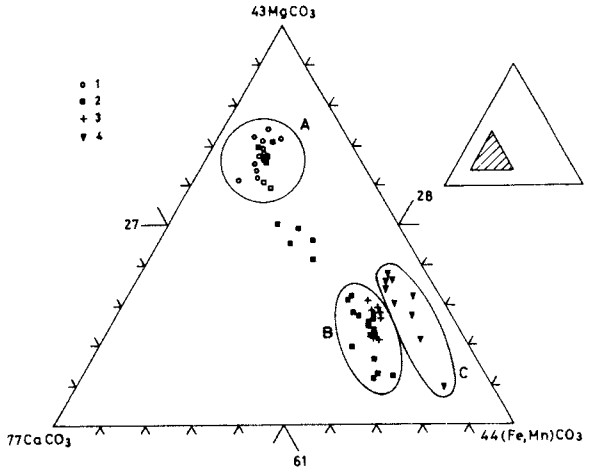

Fig. 5. $CaCO_3$-$MgCO_3$-(Fe, Mn)CO_3 ternary diagram of all ankerite analyses of samples of the Tapolcsány Metachert. Corehole DT-8. **1** — Sample 1, 139.3 m; **2** — Sample 2, 164.0 m; **3** — Sample 3, 165.3 m; **4** — Sample 5, 475.3 m. A, B, and C represent the different types of ankerites.

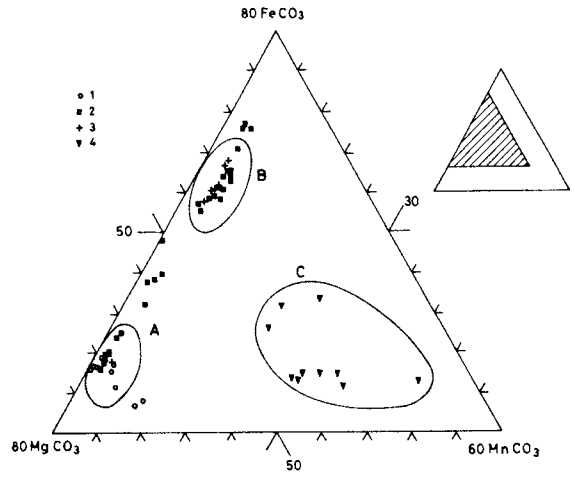

Fig. 6. $MgCO_3$-$FeCO_3$-$MnCO_3$ ternary diagram of all ankerite analyses of samples of the Tapolcsány Metachert. Corehole DT-8. 1 — Sample 1, 39.3 m; **2** — Sample 2, 164.0 m; **3** — Sample 3, 165.3 m; **4** — Sample 5, 475.3 m.

erite (up to 2.5 wt. %). The Mg content of calcite is negligible and remains below 0.15 wt. %, the detection limit. In ankerite the Fe/Mg mole ratio varies between 0.36 and 0.49, i.e. samples are poor in Fe (type A, Figs. 5, 6); the iron content fluctuates little. The Mn content increases as Fe content decreases (Fig. 6).

Most carbonates of sample No. 2 are anhedral and not zoned, (Fig. 7a), although some zoned grains occur. Among the carbonate minerals siderite, calcite, and two types of ankerite can be determined. Siderite and calcite occur as vein fillings and as grains. Small amounts of Fe, Mg, and Mn are found in calcite; the Mn concentration exceeds the concentration of iron and magnesium. The composition of ankerite is variable except for Ca, which varies within narrow limits. Based on the Fe/Mg ratios, the non-zoned ankerites are assigned to two groups (A and B). In group A the Fe/Mg mole

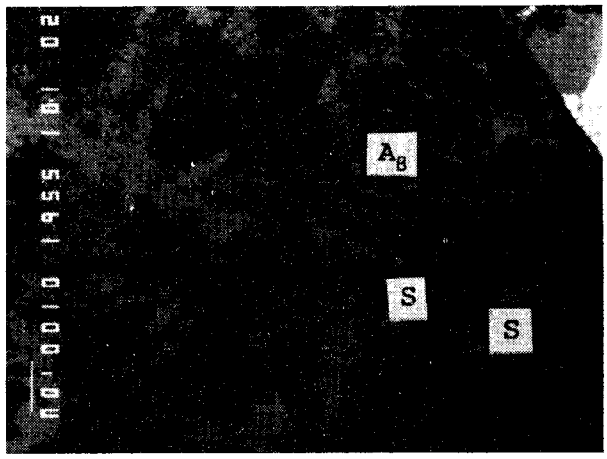

Fig. 7a. Backscattered electron image (Sample No. 2, corehole DT-8, 164.0 m). Siderite (S) and ankerite (A_B) in quartz, accompanied by sphalerite (brightest phase).

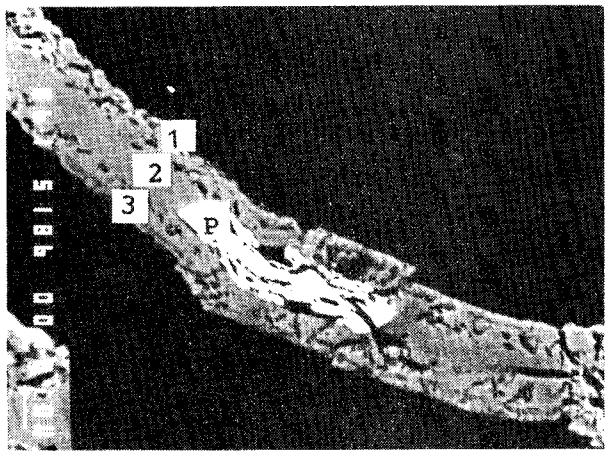

Fig. 7b. Backscattered electron image (Sample No. 2, corehole DT-8, 164 m). Pyrite (P) occurs in a siderite vein. The black groundmass is quartz. For analyses of points see Table 3.

ratio varies between 0.43 and 0.55 (iron-poor, Mg-rich ankerite, Fig. 5), whereas in group B this ratio varies between 1.22 and 2.12 (Fe-rich ankerite). The mean Mn concentration of group B samples is roughly double that of group A samples (0.93 and 0.48 wt. % respectively; Fig. 6, Tab. 3).

The Ca and Mg contents of siderites are low, 2.2 wt. % and 0.26 wt. %, respectively. In the grain-form siderite the mean Mn concentration is 0.93 wt. %. A siderite vein shows zoning, where the center is Fe-rich, Mg-, and Mn-poor (Fig. 7b). The composition of the vein center is roughly the same as that of the siderites mentioned above. Pyrite occurs locally.

The euhedral zoned, 200-300 μm sized carbonate minerals with quartz groundmass of sample No. 2 can be seen in Figs. 4a-d. Carbonate grains are not zoned where associated with pyrite, pyrrhotite, and sphalerite.

The zoned minerals of the metachert samples can be assigned to two groups:

a — In the first group ankerite, and siderite occur (Figs. 4a, b). Based on textural characteristics, siderite formed subsequent to ankerite. Fluids dissolved the parts of ankerite crys-

Table 3: Representative energy-dispersive analyses (in percent) of carbonate phases of some metachert samples of the Uppony Mountains.

No.	Sample No.	Carbonate Minerals		Ca	Mg	Fe	Mn	Range of Mn	Mean Mn	n	
				Tapolcsány Formation, Tapolcsány Metachert Member							
1.	DT-8 139.7 m	calcite		38.61	0.08	0.31	0.83	0.63-1.22	(0.85)	8	
				38.52	0.13	0.56	0.72	-	-	-	
		ankerite A**		21.41	7.88	8.36	0.21	0.17-2.52	(0.85)	14	
				22.11	7.52	6.16	2.33	-	-	-	
				21.12	8.15	8.07	0.94	-	-	-	
			zones								
2.	DT-8 164.0 m	zoned	1.	21.31	6.52	10.16	0.74	0.09-1.10	(0.71)	5	Fig. 4c
		euhedral	3.	20.55	5.73	12.71	0.09	-	-	-	
		ankerite	2.	20.08	4.70	14.34	0.90	-	-	-	
			4.	20.45	4.00	14.73	1.10	-	-	-	
			5.	20.40	3.55	16.83	0.71	-	-	-	
		zoned	s	2.22	0.26	43.03	0.99	0.42-1.33	(0.96)	5	Fig. 4b
		euhedral	3.	20.54	6.40	11.17	0.42	-	-	-	
		ankerite	4.	19.93	4.54	15.13	1.08	-	-	-	
		with side-	4.	19.84	4.72	14.94	1.33	-	-	-	
		rite core	5.	19.87	3.48	17.05	0.97	-	-	-	
		zoned	s	2.29	0.13	42.72	0.86	0.61-1.25	(0.92)	7	Fig. 4a
		euhedral	1.	20.48	6.22	11.75	0.79	-	-	-	
		ankerite	2.	20.07	4.29	15.51	1.02	-	-	-	
		with	3.	21.00	6.11	11.02	0.61	-	-	-	
		siderite	4.	19.76	4.45	14.85	1.25	-	-	-	
		rim	5.	19.74	3.74	15.75	0.89	-	-	-	
		siderite	1.p.*	2.82	0.80	41.65	1.31	0.77-1.46	(1.18)	3	Fig. 7b
		vein	2.p.	2.33	0.14	42.99	0.77	-	-	-	
			3.p.	2.47	0.65	41.13	1.46	-	-	-	
		anhedral calcite		38.94	0.06	0.38	0.62	0.13-1.00	(0.66)	5	
		anhedral		1.90	0.17	44.81	0.79	0.79-1.46	(1.01)	6	
		siderite		2.30	0.31	42.77	1.18	-	-	-	
		anhedral		19.95	4.66	14.47	1.04	0.62-1.27	(0.93)	6	
		ankerite B**		20.42	4.99	14.41	0.70	-	-	-	
				19.94	4.69	15.35	1.03	-	-	-	
		anhedral		20.75	8.36	8.72	0.44	0.44-0.53	(0.48)	6	
		ankerite A		20.94	8.20	8.12	0.24	-	-	-	
3.	DT-8 165.3 m	ankerite B		19.78	4.85	15.22	0.86	0.78-1.03	(0.90)	7	Fig. 9a
				19.69	4.93	15.31	1.02	-	-	-	
		siderite		2.14	0.37	43.88	0.85	0.51-1.10	(0.81)	8	Fig. 9a
				1.54	0.97	43.86	1.10	-	-	-	
5.	DT-8 475.3 m	Mn-rich		18.54	4.14	11.13	6.95	5.63-12.58	(8.15)	10	Fig. 9b
		ankerite		18.36	4.60	7.54	9.67	-	-	-	

* measured points; n = number of analyses; s = siderite
**ankerite A and B: explanation see in text

tals which it could reach along cracks (in Fig. 4a at edge of ankerite, in Fig. 4b at its core) and siderite precipitated in the dissolution porosity. This assumption is supported by the fact that the siderite shows no relationship with zoning in the ankerite (see later).

b — Zoned ankerite without siderite characterizes the second group (Figs. 4c, d). The zoning of grains shows a characteristic structure. At the center (the darker part in the microprobe photo) is a Mg-rich core (1st band, Figs. 4, 8), that is followed by a lighter band of several micrometers (2nd band) that is more abundant in Fe and Mn as compared to the core. Next is a band of several tens of micrometers wide with a composition that is nearly the same as that of the core (the core is somewhat poorer in Mn, Fig. 8); this is followed by a band of several micrometer (4th band) with the same composition as that of the second band. The outermost band (5th band, Figs. 4, 8; in the photo the brightest band except for that of siderite) is only rarely observed (e.g. Fig. 4a, point 5, or Fig. 4c, point 5). Compared to the earlier-formed bands this one is richer in Fe, poorer in Mn, and poorest in Mg. In all the samples the zones occur in euhedral grains, which all display the same zonal pattern. Further, within the errors of measurement, the same bands in different grains are of the same composition, and their widths vary within narrow limits. Mn accumulates mostly in bands 2 and 4 (between 0.90 and 1.33 wt. %, 1.1 wt. % mean). In decreasing order the Mn content is 0.86 wt. % in band 5, 0.60 wt. % in band 3, and 0.48 wt. % at the core. The Mn content of siderite (0.93 wt. %) is close to the mean

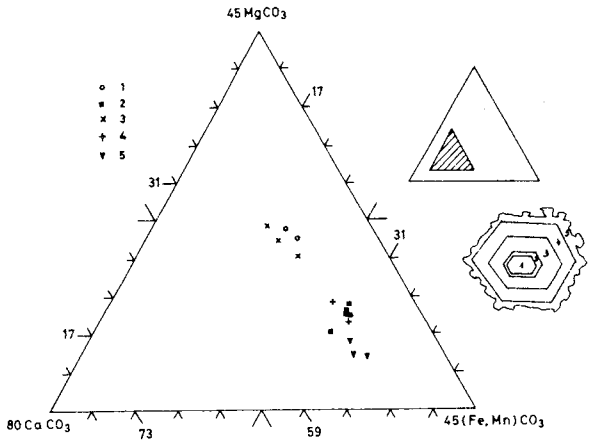

Fig. 8. $CaCO_3$-$MgCO_3$-$(Fe,Mn)CO_3$ ternary diagram of zoned ankerite analyses of sample 2 of the Tapolcsány Metachert. 1-5 zones from core to margin of euhedral crystals.

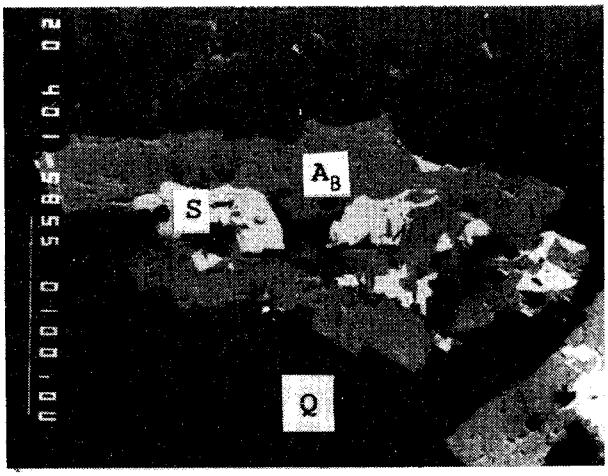

Fig. 9a. Backscattered electron image (Sample No. 3, corehole DT-8, 165.3 m); Fe-rich ankerite (A_B) and siderite (S) in quartz (Q). For analyses see Table 3.

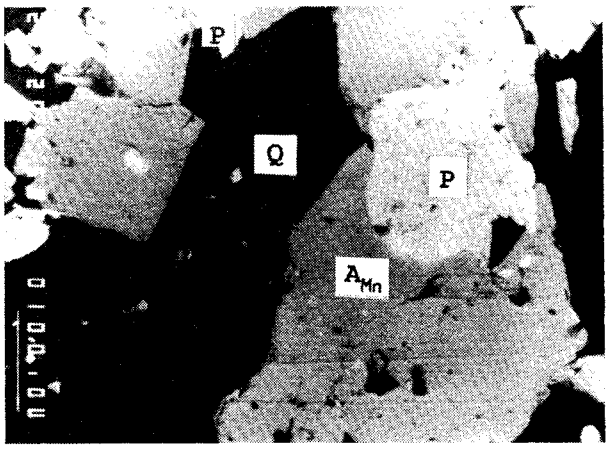

Fig 9b. Backscattered electron image (Sample No. 5, corehole DT-8, 475.3 m). Mn-rich ankerite (A_{Mn}) with quartz (Q) and pyrite (P). For analyses see Table 3.

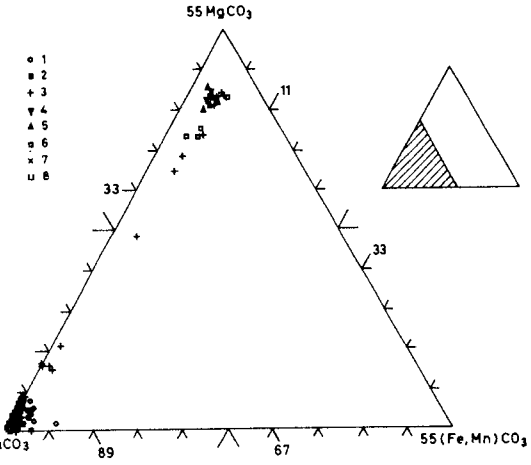

Fig. 10. $CaCO_3$-$MgCO_3$-$(Fe,Mn)CO_3$ ternary diagram of all carbonate analyses of samples of the Lázbérc Formation. Correspond 1-8 to sample numbers in Table 2.

Mn content of the ankerite bands (0.87 wt. %). Mn content varies together with Fe, except in band 5. Mg shows negative correlation with Fe + Mn (r = -0.98; Fig. 8). The average Fe/Mg mole ratio varies between 1.33 and 1.43 and is characteristic of the Fe-rich B-type ankerite, but due to zoning the scatter is large. The Ca content of the zones varies little.

In sample No. 3 Fe-rich (B-type) ankerite and siderite occur (Fig. 9a). In ankerite the Fe/Mg mole ratio varies between 1.30 and 1.68, the mean Mn content remains below 1 wt. %. The Fe content of siderite strongly fluctuates (37.97 to 43.97 wt. %) while the Mg contents are high (0.31 to 0.97 wt. %) compared to other siderites.

In the strongly pyritic groundmass of sample No. 4, both large homogeneous euhedral (70-80 μm), and small (1-10 μm) ankerite grains occur with a trace of manganese. No quantitative microprobe analysis was done on the carbonate grains of the sample.

Characteristic carbonates of sample No. 5 can be seen in Fig. 9b. These carbonate minerals differ considerably in textures and composition from those of the Tapolcsány Metachert Member discussed so far (Fig. 6). The Mn content of the carbonates is remarkable high, up to 12.6 wt. %. The Fe/Mg mole ratio varies between 0.63 and 1.17. Based on the high Mn content, it is expedient to consider it as a separate group of ankerites, C-type). The Ca content is lower, less than or equal to 18.8 wt. %. On the basis of ten carbonate ions the following formula is obtained: $Ca_{4.8}(Mg, Fe, Mn)_{5.2}(CO_3)_{10}$.

In previous samples of ankerite, the number of Ca ions falls between 4.97 and 5.44 whereas for C-type it is between 4.70 and 4.86. Consequently the Ca : (Fe + Mg + Mn) ratio is definitely lower than in all other samples (Fig. 5). Similar values were obtained by Mucci (1991) for kutnahorites from the Sterling Mine of New Jersey. Mg and Fe + Mn are negatively correlated, r = -0.73. Except for three points, the Fe contents are the same, and the variation is the result of Mg and Mn substitution for each other. Under these circumstances of uniform Fe content, the carbonate composition can be approximated by the formula: $(Ca_{3.84}Fe_{1.16})_5(Mg, Mn)_3(CO_3)_8$. With this method, the correlation between Mg and Mn is r = -0.99.

No element migration due to weathering could be identified in sample 5. The high Mn content is bound to the carbonate

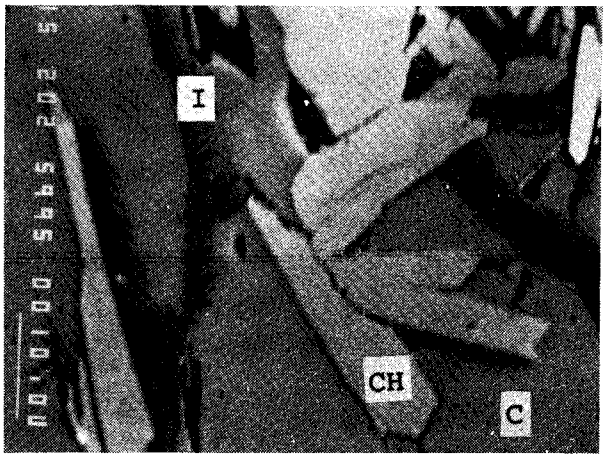

Fig. 11a. Backscattered electron image (Sample No. 1, U 450 m). Well-crystallized chlorite (CH) and illite (I) crystals in calcite (C).

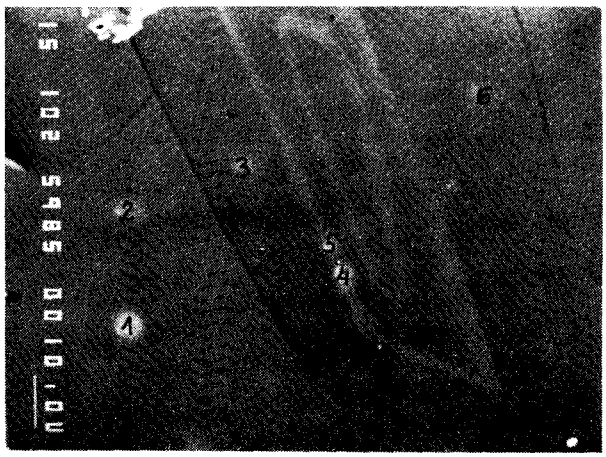

Fig. 11b. Backscattered electron image (Sample 7, U 1278 m). Mn-rich zones in calcite; for analyses see Table 4.

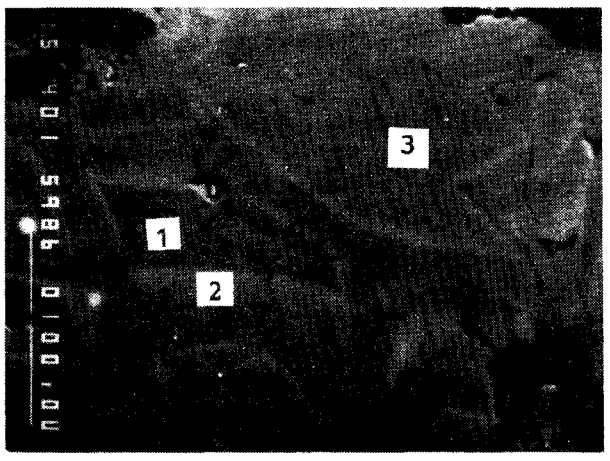

Fig. 11c. Backscattered electron image (Sample No. 7, U 1278 m). Mn-bearing zones in calcite.

phase. This can be explained by a high Mn content of the original sediment. Sample 5 is strongly enriched in quartz and based on facies analyses the original sediment probably contained some pyrite, pyrrhotite, sphalerite.

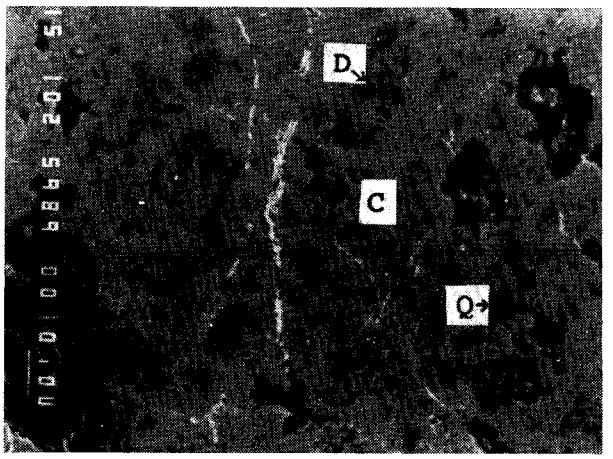

Fig. 12. Backscattered electron image (Sample No. 4, U 1050 m). Dolomite (D), quartz (Q), and subsequent vein filling with Fe-Mn-oxides (bright strips) in calcite (C).

Lázbérc Formation

In sample 1, 2 and 6 only calcite occurs (Tab. 2), in the others calcite and dolomite occur (Fig. 10). The Ca content of calcite varies between 36.9 and 39.5 wt. %, and Mg content is below 1.12 wt. % (Tab. 4). The Fe content is mostly lower than 1 wt. %, but approaches 1.5 wt. % in some samples. The mean concentration of Mn, 0.11 wt. % for all calcites analyzed, is less than that of Fe. In some samples somewhat higher Mn contents were found than the mean concentration of Mn, e.g. 0.6 wt. % in sample 3, and 1.15 wt. % in sample 7. Calcite vein networks are common and locally contain hematite scales (sample 1) and well-crystallized clay minerals (Fig. 11a). The elongate clay minerals are crudely oriented within the veins and are dispersed in the calcite.

In sample 7 calcite is zoned as the result of manganese content (Figs. 11b, c). Calcite of sample 8 is similar to that of sample 7, but zoning by manganese occurs only in one sample. Calcite vein networks are characteristic of all samples and may contain traces of Fe, Mg, and Mn.

The other carbonate phase of samples 3, 4, 5, 7, and 8 is dolomite (Figs. 12, 13a). In Fig. 13a a second generation calcite is seen in the fractured dolomite. Clay-mineral-bearing Fe-rich areas occur locally in the dolomite. The Ca/Mg mole ratio varies between 1.07 and 1.42; the Ca proportion is slightly enriched over stochiometric dolomite. In one sample a carbonate transitional between calcite and dolomite can be observed (Figs. 10, 13b). In Fig. 13b a skeletal dolomite crystal can be seen with smaller dolomite grains inside and outside the crystal, all of which are surrounded by calcite. The Fe-Mn oxide (oxyhydroxide?) precipitation parallel to the dolomite skeletal crystal faces may indicate the front line of calcitization since the Fe-Mn-binding capacity of calcite is weaker than that of the dolomite. Dolomite-rich rocks are enriched in Fe and Mn, containing mean contents of 1.55 wt. % Fe and 0.4 wt. % Mn. The Mn concentration exceeds 1 wt. % in several samples. The Mg content varies between 9.77 and 11.8 wt. % in dolomite.

Fe-Mn oxide weathering products occur in the calcite, indicating that the calcite may also be secondary. In sample 4, the Mg is leached along the fracture network due to weathering.

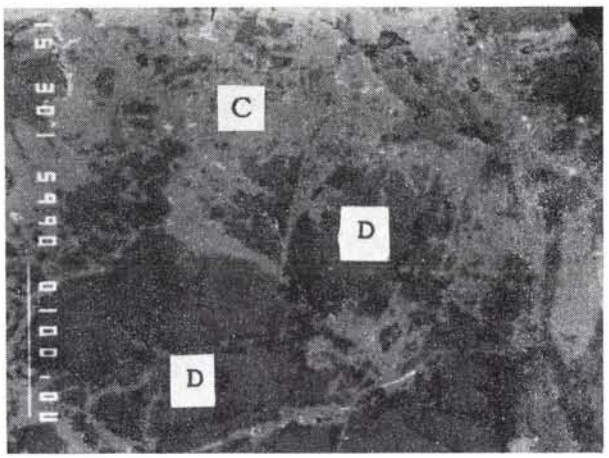

Fig. 13a. Backscattered electron image (Sample No. 4, U 1050 m). Analyses of dolomite (D) and calcite (C) are found in Table 4.

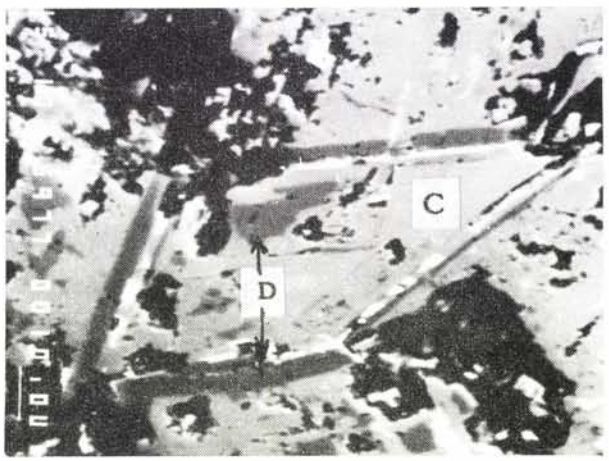

Fig. 13b. Backscattered electron image (Sample No. 8, U 1279 m). Dolomite (D) zone in calcite (C). For analyses see Table 4.

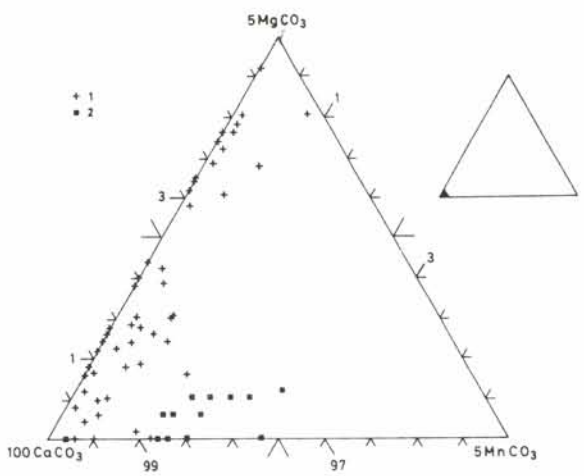

Fig. 14. $CaCO_3$-$MgCO_3$-$MnCO_3$ ternary diagram of calcite analyses of the Tapolcsány Metachert and of the Lázbérc Formation. **1** — Lázbérc Formation; **2** — Tapolcsány Metachert.

Part of limestone samples 4 to 8 show common effects of weathering manifested by Fe-oxide, and Fe-Mn-oxide-bearing dispersed phases and vein fillings (Fig. 12). These weathering products are heterogeneous, the Fe-oxide and Fe-Mn-oxide occur with the very fine-grained mixture of clay and carbonate minerals.

Discussion

Formation of the carbonate phases

The process of formation of the zoned ankerite of sample No. 2 is best understood, thus only this phase will be dealt with in detail.

Zoned ankerite formed from a fluid of changing composition, either during a single episode or during several episodes. Zoned ankerite may form by diagenetic, metamorphic, metasomatic, or detrital processes. Their euhedral shape and jagged edges, however preclude a detrital origin.

Detrital quartz is cemented by zoned ankerite. Carbonate formed as a cement. Locally the margins of carbonate grains are "dendritic", characteristic of the growth of carbonate around the quartz (quartz grains are quasi piled up at the edges of carbonate crystals). Thus, quartz was disseminated in calcite during growth of the carbonate grains as shown in Fig. 4a where some quartz grains disturb the boundary between bands 3 and 4.

Their euhedral shape can be explained both by metamorphic, diagenetic, and metasomatic processes. In the course of metamorphism usually larger more homogeneous grains develop from the smaller carbonate grains. With this process zoning may develop by diffusion. In sample 2, however oscillation zoning can be observed with sharp zone boundaries that cannot be explained by diffusion. Further, the carbonate crystals are not oriented, but are dispersed, which does not support a metamorphic origin.

We propose that the zoned ankerite is of metasomatic origin. Small carbonate crystals developed in the original sediment during diagenesis. Subsequent to diagenesis (Árkai 1983) the sediment was affected by metasomatic fluids, promoted the growth of ankerite crystals on the pre-existing carbonate seeds. The composition of the fluids changed from time to time causing the zonation. The growing carbonate crystals concentrated the quartz grains around them and some of the quartz grains were dissolved. Some detrital quartz grains were cemented by the carbonate.

Summary

Mn content characterizes the metachert samples while Mg content characterizes the limestone samples.

1 — The mean Mn content of the analyzed carbonate phases is higher in the metachert than in the limestone samples; the Mn content of calcite exceeds both the Fe and Mg contents; and the very high Mn content of sample No. 5, all indicate that the original sediment had a high Mn content. In contrast the limestone-dolomite formed under more oxidative conditions and is not characterized by high primary Mn content.

2 — The Fe-Mg metasomatism of the metachert is supported by the occurrence of euhedral carbonate minerals (ankerite and siderite) showing Fe-Mg zoning and by the occur-

Table 4: Representative energy-dispersive analyses (in percent) of carbonate phases of some limestone samples of the Uppony Mountains.

No.	Sample No.	Carbonate Minerals		Ca	Mg	Fe	Mn	Range of Mn	Mean Mn	n	
				Lázbérc Formation							
1.	U 450 m	calcite		38.32	0.45	0.86	0.13	0.00-0.19	(0.07)	9	
2.	U 470 m	calcite		38.60	0.34	0.81	0.10	0.10-0.37	(0.24)	7	
3.	U 1010 m	calcite		39.23	0.00	0.45	0.12	0.00-0.58	(0.32)	11	
		dolomite		21.40	11.35	1.36	0.45	0.09-0.52	(0.40)	5	
4.	U 1050 m	calcite		38.43	0.35	0.72	0.11	0.00-0.20	(0.16)	7	Fig. 13a
		dolomite		21.68	11.28	1.49	0.52	0.13-0.52	(0.29)	5	Fig. 13a
5.	U 1060 m	calcite		38.70	0.30	0.11	0.00	0.00-0.15	(0.08)	2	
6.	U 1090/b m	calcite		39.09	0.18	0.47	0.07	0.07-0.41	(0.25)	5	
7.	U 1278 m	Mn-zoned calcite	1.p.*	37.47	1.07	0.00	0.00	0.00-1.15	(0.47)	6	Fig. 11b
			2.p.	37.93	0.61	0.07	0.27	-	-	-	
			3.p.	38.47	0.83	0.13	0.26	-	-	-	
			4.p.	37.79	0.56	0.00	1.13	-	-	-	
			5.p.	37.43	0.70	0.00	1.15	-	-	-	
			6.p.	38.18	0.63	0.22	0.00	-	-	-	
		calcite		38.48	0.22	1.01	0.01	0.00-0.91	(0.14)	14	
		dolomite		22.92	10.48	1.70	0.55	0.24-0.63	(0.48)	5	
8.	U 1279 m	calcite		38.26	0.89	0.17	0.00	0.00-0.33	(0.19)	5	Fig. 13b
		dolomite		20.95	11.75	2.19	0.35	0.17-0.52	(0.39)	8	Fig. 13b
		transition		36.01	1.99	0.92	0.04	0.00-0.52	(0.20)	7	
		from calcite		35.88	2.21	0.05	0.00	-	-	-	
		into dolomite		35.63	2.18	0.47	0.10	-	-	-	
		(dedolomitization)		34.61	2.77	0.46	0.10	-	-	-	
				28.54	6.59	1.47	0.28	-	-	-	
				25.23	8.94	1.49	0.52	-	-	-	
				24.50	9.48	1.53	0.37	-	-	-	

* measured points, which are indicated on Fig. 11b, n = number of analyses

Table 5: Comparison of the characteristics of two Uppony manganese deposits.

	Tapolcsány Metachert Member					**Lázbérc Formation**	
original sediment	sedimentary rock of euxine facies and of high primary pyrite and organic matter content					limestone of carbonate platform facies (more oxidative facies)	
manganiferous carbonate phases	calcite	siderite	ankerite A	ankerite B	Mn-rich ankerite (sample No. 5)	calcite	dolomite of low Fe-content
average Mn-content of carbonate phases (wt. %)	0.76	0.97	0.67	0.93	8.15	0.21	0.39
element ratios	Mn > Fe, Mg in all measured samples	-	Fe/Mg mole ratio 0.36-0.55	Fe/Mg mole ratio 1.22-2.12	-	two types: a) stochiometric b) Fe, Mg, Mn in traces, Fe > Mn in all samples, except Mn-zoning (samples 7 and 8)	Ca/Mg mole ratio 1.07-1.42, dolomitization, dedolomitization process
			In the Mn-rich ankerite of sample No. 5 the Fe/Mg ratio varies between 0.63 and 1.17 but is displaced towards the Fe-rich members			$\overline{Mn} < \overline{Fe}$	
			$\overline{Mn}_{ankerite\ A} < \overline{Mn}_{ankerite\ B}$			Mn, $Fe_{calcite}$ < Mn, $Fe_{dolomite}$ Except in zoned calcite	
other features	Euhedral zoned ankerites, ankerite-siderite phases, as well as the carbonate assemblage of varied composition reflect non-equilibrium state. Manganiferous carbonates fill the micropores of the rock. The high Mn-concentration of sample No. 5 is found in carbonate phase and is probably due to the higher Mn-content of the original sediment. Metasomatism was subsequent to weak metamorphism, orientation of grains cannot be seen in the carbonates.					With Mn zoning the Mg-content is somewhat higher while the Fe-content is slightly lower.	Dolomitization and dedolomitization resulted in heterogeneous dolomite with less Fe and even less Mn.

Weathering (surficial effects)

Fe-Mn-oxide precipitation (manganite; Balogh & Pantó 1954)

manganiferous shale — different basement rocks — manganiferous spar iron ore

$\overline{Mn}$: 0.83 wt. % $\overline{Mn}$: 0.30 wt. %

rence of ankerite phases of different compositions (types A, B, and C); in the limestone- dolomite section, metasomatism is supported by the process of ferrous-dolomitization.

3 — Ankerite can be compared with ferrous dolomite where the Fe/Mg mole ratio varies around 1 : 1. The Fe/Mg ratio shows a fluctuation in the zoned carbonate minerals and in the unzoned ankerite phases. Three main ankerite groups are distinguished (Table 3).

In group A the Fe/Mg mole ratio is 0.43 to 0.81, which is an Fe-poor, Mg-rich type.

In group B the Fe/Mg mole ratio varies between 1.22 and 2.12, an Fe-rich variety.

In group C the Mn content is high and the phase can be interpreted as a transitional member between dolomite and kutnahorite; the Fe/Mg mole ratio varies between 0.63 and 1.17. This type of carbonate is characteristic of rocks that underwent regional metamorphism or metasomatic processes (Mucci 1991).

As a whole, the composition of carbonate minerals is extremely heterogeneous, which reflects the changing composition of the metasomatic fluids as a function of time; the process did not reach equilibrium.

Whether metasomatism increased the Mn content or what other kinds of changes in the Mn distribution it caused, cannot be unambiguously determined. The manganiferous siderite of the metacherts, the greater Mn content of the Fe-rich B-type ankerite, as well as the observation that in certain samples the Mn content increases in parallel with the increase of Fe, reflect the metasomatic origin of a part of the Mn content.

In the limestone samples, the Mn zoning observed in calcite as well as the higher Mn content of the ferrous dolomite reflect the metasomatic process as a source of Mn.

Weathering leached Fe and Mn from the carbonate minerals and resulted in the precipitation of Fe-Mn oxides. In the Lázbérc Formation and the Tapolcsány Metachert, surficial Fe-Mn concentrations are different in the limestone and metachert, sparite iron ore and manganiferous shale (Table 5). In spite of the different occurrences, the source of Mn as well as the process of accumulation were the same. In the Lázbérc Formation, on the basis of textural features, the weathering resulted in dedolomitization (Fig. 14; Mg-dissolution, calcitization; Theriault & Hutcheon 1987).

Acknowledgements: Authors are indebted to Gyorgy Pantó, and Páter Árkai, and James R. Hein for critical review of the paper. Gábor Dobosi and Géza Nagy kindly aided in computer data processing. James R. Hein improved the English. Work completed in conjunction with IGCP Project 318.

References

Árkai P., 1978: Key section of the Uppony Mountains). Research report, manuscript (in Hungarian).

Árkai P., (1983): Very low- and low-grade alpine regional metamorphism of the Paleozoic and Mesozoic formation of the Bükkium, NE-Hungary. *Acta Geol. Hun.*, 26, 1-2, 83-101.

Árkai P., Horváth Z., Tóth M., 1981: Transitional very low- and low-grade regional metamorphism of the Paleozoic formations, Uppony Mountains, NE-Hungary: Mineral assemblages, illite-crystallinity, -b_0 vitrinite reflectance data. *Acta Geol. Acad. Sci. Hung.*, 24, 2-4, 265-294.

Balogh K., 1964: Geological formations of the Bükk Mountains. *Annals of the Hung. Geol. Survey*, 48, 243-719 (in Hungarian).

Duncumb P. & Jones E.M., 1969: Report No. 260: Electron probe microanalysis: an easy-to-use computer program for correcting quantitative data. *Tube Investments Research Laboratories, Hinxton Hall*, Hinxton, Saffron Walden, Essex.

Hem J.D., 1972: Chemical factors that influence the availability of iron and manganese in aqueous systems. *Geol. Soc. Amer. Bull.*, 83, 443-450.

Kiss J., 1958: Ore geological studies at the Darnó Hill. *Földt. Közl.*, 88, 27-41 (in Hungarian).

Koch S., Grasselly Gy. & Donáth É., 1950: Minerals of iron ore occurrences in Hungary. *Acta Mineral. Petrogr., (Szeged)*, 1-41 (in Hungarian).

Kovács S., 1984: Lithostratigraphic units of the Uppony Mountains. *Manuscript* (in Hungarian).

Kozur H. & Mock R., 1973: Zum Alter und zur tektonischen Stellung der Meliata-Serie. *Geol. Zbor. Geol. Carpath.*, 24, 365-374.

Mucci A., 1991: The solubility and free energy of formation of natural kutnahorite. *Canad. Mineralogist*, 29, 113-121.

Nagy G. & Fórizs I., 1986: Experiences on microprobe quantitative analyses carried out by EDS. *XXIX Hung. Annual Conf. on Spectral Analysis, Keszthely, Abstracts*, 257-261 (in Hungarian).

Pantó G., 1948: Structural and ore mineralization observations on the iron ore range of Rudabánya. *Annual Report of the Hung. Geol. Survey, X. Report* (in Hungarian).

Pantó G., 1954: Mining geological mapping in the Uppony Mountains. *Annual Report of the Hung. Geol. Survey*, 910 (in Hungarian).

Pantó G., 1956: Geological structure of the iron ore range of Rudabánya. *Annals of the Hung Geol. Survey*, XLIV, 327-490 (in Hungarian).

Theriault F. & Hutcheon I., 1987: Dolomitization and calcitization of the Devonian Grosmont Formation, Northern Alberta. *J. Sed. Petrology*, 57, 955-966.